Title	Electrical activation of high-concentration aluminum implanted in 4H-SiC
Author(s)	Negoro, Y; Kimoto, T; Matsunami, H; Schmid, F; Pensl, G
Citation	Journal of Applied Physics (2004), 96(9): 4916-4922
Issue Date	2004-11-01
URL	http://hdl.handle.net/2433/24194
Right	Copyright 2004 American Institute of Physics. This article may be downloaded for personal use only. Any other use requires prior permission of the author and the American Institute of Physics.
Type	Journal Article
Textversion	publisher; none

Electrical activation of high-concentration aluminum implanted in 4H-SiC

Y. Negoro, T. Kimoto, and H. Matsunami
Department of Electronic Science and Engineering, Kyoto University, Kyotodaigaku-katsura, Nishikyo, Kyoto 615-8510, Japan

F. Schmid and G. Pensl
Institut für Angewandte Physik, Universität Erlangen-Nürnberg, DE-91058 Erlangen, Germany

(Received 17 May 2004; accepted 2 August 2004)

High-dose aluminum-ion (Al^+) implantation into 4H-SiC (0001) and $(11\bar{2}0)$ has been investigated. The dependences of the electrical properties on the implanted Al^+ dose and on the annealing time were examined by Hall-effect measurements. A low sheet resistance of 2.3 $k\Omega/\square$ (0.2 μm deep) was obtained in a (0001) sample by implantation of Al^+ with a dose of 3.0×10^{16} cm^{-2} at 500 °C and a subsequent high-temperature anneal at 1800 °C for a short time of 1 min. In the case of $(11\bar{2}0)$ samples, even room-temperature implantation resulted in a low sheet resistance of 2.3 $k\Omega/\square$ (0.2 μm-deep) after anneal at 1800 °C. The Hall data are compared with the calculated values determined by using the doping-concentration dependent ionization energy of Al acceptors. The experimentally obtained free-hole concentrations agree well with the theoretically expected values. Hole mobilities are not as high as the empirical mobilities obtained in Al-doped epitaxial layers. The differences in the electrical properties between the experimental data and expected values are discussed. © *2004 American Institute of Physics*. [DOI: 10.1063/1.1796518]

I. INTRODUCTION

Silicon carbide (SiC) is an attractive semiconductor material for high-power electronic devices. However, the device processing in SiC is one of crucial issues to realize high-performance devices. For example, selective doping can only successfully be conducted by ion implantation because of the low diffusion coefficients of dopants.[1] In order to form selective *p*-type regions in SiC, implantation of aluminum ions (Al^+) or boron-ions (B^+) is commonly used. Al is particularly attractive to form heavily doped p^+-regions with reasonable sheet resistance, because Al acceptors have a smaller ionization energy (190 meV, Ref. 2) than B acceptors (285 meV) Ref. 3 in 4H-SiC. The use of B^+ implantation is effective to form deep *p-n* junctions because B atoms reach larger projected ranges due to their lighter mass. In many device applications, localized n^+- and p^+-type regions leading to low contact resistances are fundamental requirements. In the case of n^+-type region, implantation of phosphorus ions (P^+) has attracted increasing attention[4] and resulted in a very low sheet resistance of about 50 $\Omega/\square$.[5,6] On the other hand, high-dose Al^+ implantations are usually employed for forming p^+ regions. The high-dose Al^+ implantation, however, introduces a high density of defects in the implanted region.[7] Ion implantation at an elevated temperature (hot implantation) Ref. 8 and post-implantation annealing at a high temperature[3,9] are, therefore, necessary to reduce the implantation-induced damages. Despite these processing steps, the Al^+ implantation is still a major obstacle to the SiC processing technology, because of its high sheet resistance of 5–10 $k\Omega/\square$.[10,11] It is not clear yet whether this high sheet resistance is due to an incomplete electrical activation of the Al acceptor or to a low hole mobility which is strongly reduced by scattering centers. As a consequence, it has not been seriously discussed whether the resistance of 5–10 $k\Omega/\square$ is the optimal value, which is determined by theoretical limits.

The 4H-SiC $(11\bar{2}0)$ face, which is perpendicular to the (0001) face, has recently shown a series of promising properties such as a superior metal-oxide-semiconductor (MOS) interface[12] and a low sheet resistance of phosphorus (P^+)-implanted *n*-type regions.[13,14] Furthermore, remarkable lattice recovery[15] and an excellent surface flatness could be realized in high-dose P^+-implanted $(11\bar{2}0)$ samples.[14] Up to now, no results have been reported on high-dose Al^+ implantation into the $(11\bar{2}0)$ face of 4H-SiC.

In this paper, high-dose Al^+ implantations into (0001) and $(11\bar{2}0)$ faces of 4H-SiC are systematically investigated. The dependence of electrical properties on implanted Al^+ dose and annealing time are examined by Hall-effect measurements. Our experimental Hall data are compared with values calculated on the basis of the Boltzmann approximation and by using the Al ionization energy which depends on the doping concentration. Differences between experimental data and expected theoretical values are discussed.

II. EXPERIMENTS

The starting substrates are 8° off-axis *n*-type 4H-SiC (0001) and on-axis *n*-type 4H-SiC $(11\bar{2}0)$ purchased from Cree or Nippon Steel Co. Nitrogen-doped (*n*-type) 4H-SiC epilayers are grown on the substrates by chemical vapor deposition (CVD) at Kyoto University. The net donor concentration of epilayers was about 1×10^{16} cm^{-3}. Multiple implantation of Al^+ was carried out either at 500 °C or at room temperature (RT) to form a 0.2 μm deep box profile of Al. The implantation energies and the corresponding ratio of the doses were 160, 100, 60, 30, 10 keV and 0.51, 0.21, 0.15,

0.09, 0.04, respectively. The total dose was varied from 4×10^{15} cm^{-2} to 6×10^{16} cm^{-2}, which corresponds to the Al concentration of 2×10^{20} cm^{-3}–3×10^{21} cm^{-3}. Part of the samples was coimplanted with carbon (C^+): the C^+ dose was 20% or 100% dose of implanted Al^+ dose. The coimplantation of C atoms is expected to increase the electrical activation of Al acceptors.[3] Excess C interstitials effectively raise the probability for Al atoms to occupy Si sublattice sites where they act as a shallow acceptors.[16]

After forming a graphite cap on the whole surface of implanted samples,[17] postimplantation annealing was performed in an Ar ambient at 1800 °C for 1–180 min using a CVD reactor. The graphite cap suppresses surface roughening during the high-temperature annealing. It was successfully removed in an O_2 ambient at 900 °C for 30 min;[17] by this process only a weak oxidation of the SiC surface takes place.

The electrical properties of Al^+-implanted regions were characterized by Hall-effect measurements in the temperature range from 180 K to 830 K using the van der Pauw configuration. To avoid leakage current along the sample edges under the measurements, clover-leaf shaped mesa structures (about 4×4 mm^2) were prepared by reactive ion etching. Ohmic contacts in the van der Pauw arrangement were formed by thermal evaporation of Ti (5 nm) and Al (100 nm) and subsequent annealing at 950 °C for 1 min.

III. RESULTS & DISCUSSION

A. Dependence of the electrical properties on the implant dose and the annealing time

Figure 1 shows the dependence of (a) free-hole concentration and (b) sheet resistance (resistivity) at RT on the implanted Al^+ dose for (0001) and $(11\bar{2}0)$ samples. The annealing time for (0001) and $(11\bar{2}0)$ was 30 min and 5 min, respectively. The free-hole concentration was obtained from the measured Hall coefficient, assuming a Hall scattering factor of 1.0. Up to 3×10^{16} cm^{-2}, the free-hole concentration increases with increasing implanted Al^+ dose in (0001) samples, resulting in the maximum value of 3×10^{19} cm^{-3}. When the implanted Al^+ dose exceeds 3×10^{16} cm^{-2}, the hole concentration turns to decrease, probably due to a higher density of residual compensating defects introduced by the higher implanted Al^+ dose. In the case of Al^+ and C^+ coimplantation (20% of Al^+ dose), the free-hole concentration is higher by a factor of 1.5–2.5 compared to the samples which are only implanted with Al^+ at the same dose. This result supports the observation of Troffer *et al.*[16] that C^+ coimplantation enhances the probability for Al atoms to occupy Si sublattice sites. At the highest implanted Al^+ dose of 6×10^{16} cm^{-2}, effects of C^+ coimplantation are very small. The increased dose of C^+ may generate more defects and result in the strongly decreased free-hole concentration. The data shown here will be compared to the values theoretically expected in Sec. III C.

In the case of $(11\bar{2}0)$ samples, the free-hole concentration increases with increasing implanted Al^+ dose, and does not turn to decrease even at the highest dose of 6.0

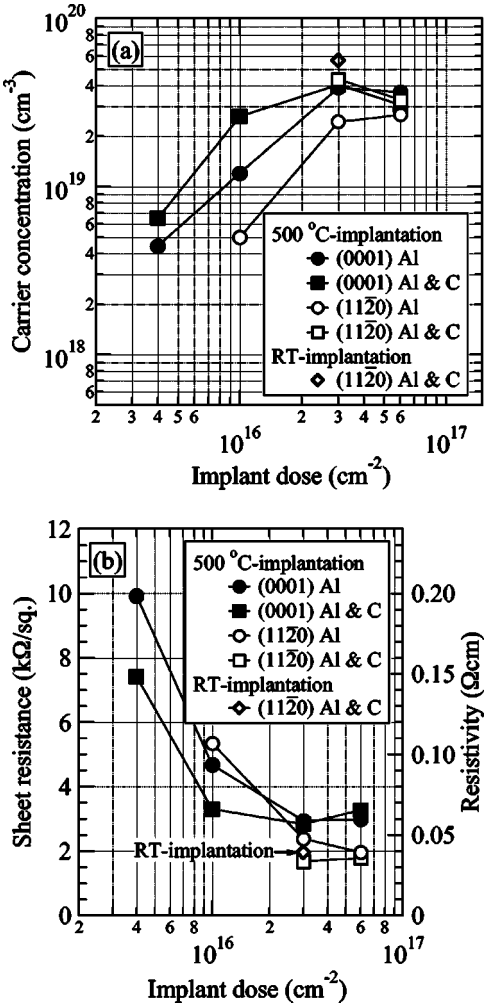

FIG. 1. Al^+-dose dependence of (a) free-hole concentration and (b) sheet resistance (resistivity) for 4H-SiC (0001) and $(11\bar{2}0)$ obtained from Hall-effect measurements at RT.

$\times10^{16}$ cm^{-2}. However, the free-hole concentration of $(11\bar{2}0)$ samples at each dose is smaller than that of (0001) samples. This may be partly due to the difference of electrical conduction mechanism including impurity-band conduction in $(11\bar{2}0)$ and (0001) samples, which will be discussed later and/or to out-diffusion of Al atoms in $(11\bar{2}0)$ samples during the high-temperature annealing.

Figure 2 shows the Al depth profiles for (0001) and $(11\bar{2}0)$ samples after annealing determined by SIMS measurements. Both out-diffusion of Al close to the surface and in-diffusion of Al from the implantation-tail region to the bulk region were observed for $(11\bar{2}0)$ even after a 5 min annealing at 1800 °C, although the implanted Al box profile was unchanged after the annealing for 30 min in the case of (0001) sample. The observed change in the implanted profile is caused by diffusion of Al atoms toward the $\langle11\bar{2}0\rangle$ direction, which is more significant than toward the $\langle0001\rangle$ direction.[18] By employing C^+ coimplantation for $(11\bar{2}0)$ samples, the diffusion of Al atoms was less pronounced. At the same time, the free-hole concentration in C^+ coimplanted $(11\bar{2}0)$ samples becomes higher than in only Al^+ implanted

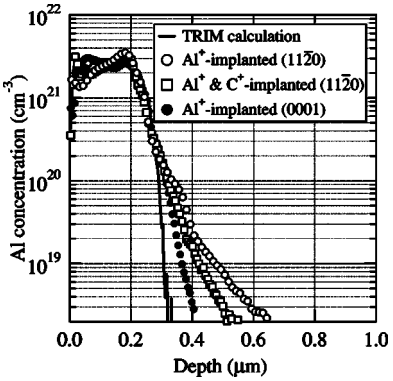

FIG. 2. Depth profile of implanted Al atoms measured by SIMS. The solid line depicts the profile calculated by TRIM as a reference.

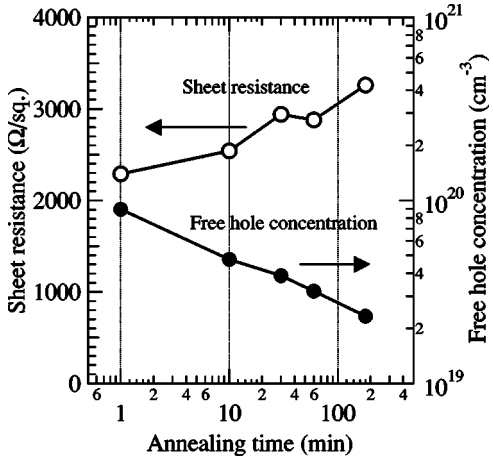

FIG. 3. Annealing-time dependence of sheet resistance and free-hole concentration for Al^+-implanted SiC (0001) with a dose of 3.0×10^{16} cm^{-2}.

(11$\bar{2}$0) samples. A high free-hole concentration of 5.7 $\times10^{19}$ cm^{-3} could be obtained in a (11$\bar{2}$0) sample by C^+ coimplantation even at RT.

As is shown in Fig. 1(b), the sheet resistance of Al^+-implanted (0001) annealed at 1800 °C for 30 min takes a minimum value of 2.9 kΩ/□, at an implanted dose of 3.0×10^{16} cm^{-2}. This value is comparable to the best value in a recent report.[19] The sheet resistance of (0001) samples turns to increase, when the implanted dose exceeds 3.0×10^{16} cm^{-2}. This is attributed to the decrease of the free-hole concentration shown in Fig. 1(a). When C^+ coimplantation was employed, the sheet resistance was reduced by 5% to 20% compared to the corresponding Al^+ implanted samples.

For (11$\bar{2}$0) samples, the sheet resistance could be reduced down to 1.9 kΩ/□ by increasing the implanted Al^+ dose up to 6.0×10^{16} cm^{-2}. A further decrease of the sheet resistance was obtained by C^+ (100% of Al^+ dose) coimplantation. The sheet resistance of 1.7 kΩ/□ achieved by the coimplantation of 3.0×10^{16} cm^{-2} for Al^+ and 3.0×10^{16} cm^{-2} for C^+ is the lowest value ever reported in *p*-type 4H-SiC. It should be noted that a low sheet resistance of 1.9 kΩ/□ could be achieved even by RT implantation. It is well recognized that high-dose Al^+ implantations into SiC (0001) samples always lead to insufficient results because the recrystallization of a highly-damaged region never reproduces homogeneously the original SiC polytype. It is, therefore, remarkable that the lattice recovery in the RT-implanted (11$\bar{2}$0) sample[14] results in the low resistance as shown in Fig. 1(a). From the view of device process technology, this result is very attractive because RT implantation has an advantage of higher productivity than hot implantation.

Figure 3 shows the annealing-time dependence of sheet resistance and free-hole concentration for Al^+-implanted (0001) with a dose of 3.0×10^{16} cm^{-2}. The annealing temperature was fixed at 1800 °C. The free-hole concentration gradually decreases with increasing annealing time. A maximum hole concentration of 8.9×10^{19} cm^{-3} was achieved by 1 min annealing. Correspondingly, a minimum sheet resistance of 2.3 kΩ/□ was obtained from the short-time annealing. The decrease of free-hole concentration with increasing the annealing time is not due to a decrease of Al atoms, because no out-diffusion of Al atoms during high-temperature annealing was found in the (0001) samples as observed in Fig. 2. In order to understand this annealing-time behavior, cross-sectional transmission electron spectroscopy (XTEM) analyses were carried out. Figures 4(a) and 4(b) show the XTEM images for Al^+-implanted (0001) samples annealed for 1 min and 180 min, respectively. The XTEM images were taken from the [1$\bar{2}$10] direction. These images indicate that the amount of residual defects for the 1 min annealed sample and the 180 min annealed sample is comparable. A relatively high density of stacking faults (SFs) (about 30 SFs in the 0.2 μm thick implanted region) is observed in both samples. A difference between two images could only be found near the implantation-tail region (about 0.25 μm from the surface). The density of defects remains higher near the edge for the 1 min annealed sample than for

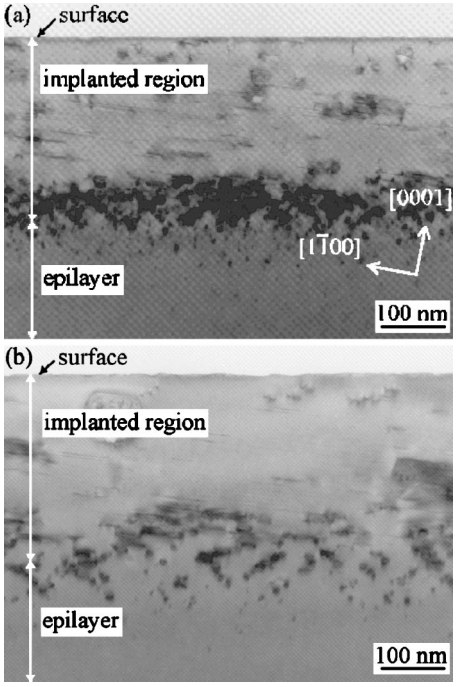

FIG. 4. Cross-sectional TEM images of Al^+-implanted (0001) annealed for (a) 1 min and (b) 180 min taken from the [1$\bar{2}$10] direction. Implant dose for each sample is 3.0×10^{16} cm^{-2}.

the 30 min annealed sample. These defects near the tailing edge of implanted region, however, may not affect the electrical activation of implanted Al atoms within the box-profile region. The longer annealing time probably generates secondary defects, which cannot be detected by TEM.

Our investigations of high-dose Al^+-implantation can be summarized as follows: Sheet resistances of $(11\bar{2}0)$ take smaller values than that of (0001), when high-dose implantation at RT or extremely high-dose (6×10^{16} cm^{-2}) implantation at 500 °C is employed, because only the $(11\bar{2}0)$ samples can be remarkably recrystallized under such implantation conditions. Another feature is that the sheet resistance of $(11\bar{2}0)$ and (0001) are comparable, when implantation is employed at 500 °C and implant dose is below 3×10^{16} cm^{-2}.

B. Temperature dependence of electrical properties

Hall-effect measurements from 180 K to 820 K were conducted for Al^+/C^+ coimplanted (0001) and $(11\bar{2}0)$ samples. Implanted Al^+ and C^+ doses for both samples are 3.0×10^{16} cm^{-2} and 6.0×10^{15} cm^{-2}, respectively. Annealing was employed at 1800 °C for 10 min. Figure 5(a) shows the free hole concentration as a function of the reciprocal temperature for (0001) and $(11\bar{2}0)$. The solid curve represents the effective density of states in the valence band, calculated using the hole effective mass reported by Son *et al.*[20] The temperature dependence of free hole concentration for (0001) is weak even at high temperatures, reflecting a feature of degenerated semiconductor. For $(11\bar{2}0)$, the hole concentration is almost constant in the temperature range below RT, indicating that the $(11\bar{2}0)$ sample becomes degenerated below RT. It is not yet fully understood why the free-hole concentration in $(11\bar{2}0)$ is lower than that in (0001). The lower concentration may be partly due to out-diffusion of Al atoms during high-temperature annealing as mentioned above. Besides the out-diffusion, some other factors might affect the lower hole concentration. Because the degree of compensation in the two samples might be different, it is expected that the onset of impurity-band conduction might occur at different temperature. It seems that the compensation in the (0001) sample is higher than that in the $(11\bar{2}0)$ sample. Consequently there are more empty sites in the impurity band for the (0001) sample, which may cause that impurity-band conduction dominates the transport of holes in almost the whole temperature range investigated, leading to the temperature-independent free-hole concentration. In the $(11\bar{2}0)$ sample, the conduction in the valence band dominates at temperatures above RT.

Figure 5(b) shows the temperature dependence of Hall mobility (hole) for the (0001) and $(11\bar{2}0)$ samples. The mobility in the $(11\bar{2}0)$ sample takes a value of 10 cm^2/Vs at RT, which is about three times higher than that in the (0001) sample. The remarkable lattice recovery in the implanted $(11\bar{2}0)$ sample[13,14] may be responsible for the much higher mobility than in the (0001) sample.

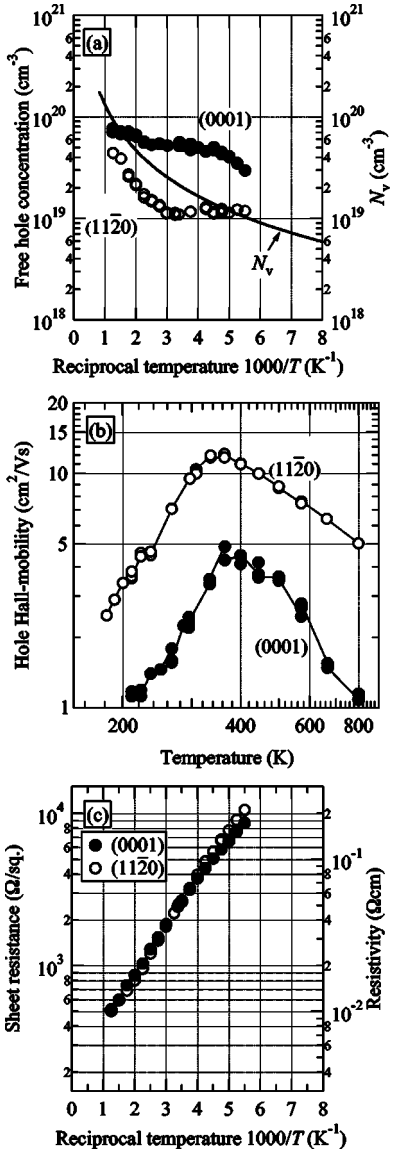

FIG. 5. Temperature dependence of (a) free-hole concentration, (b) hole Hall mobility, and (c) sheet resistance (resistivity) for 4H-SiC (0001) and $(11\bar{2}0)$ implanted with an Al^+ dose of 3.0×10^{16} cm^{-2} and a C^+ dose of 6.0×10^{15} cm^{-2}, obtained from Hall effect measurements. Postimplantation annealing was carried out at 1800 °C for 10 min.

The temperature dependence of sheet resistance (resistivity) is shown in Fig. 5(c). In the whole temperature range investigated in this study, the sheet resistance (resistivity) of these particular (0001) and $(11\bar{2}0)$ samples is almost the same, which means that the higher hole mobility of the $(11\bar{2}0)$ sample is canceled by the lower free-hole concentration.

C. Discussion of the electrical properties in p^+-SiC

For the optimization of SiC-based devices, it is very important to understand the difference between the experimentally determined parameters shown above and the electrical properties theoretically expected. In order to calculate the free-hole concentration for a wide concentration range of acceptors, the ionization energy of Al acceptors, which depends on the acceptor concentration, has to be known. Several

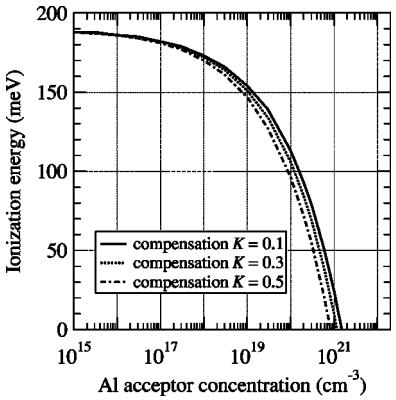

FIG. 6. Calculated ionization energy of Al acceptor in 4H-SiC as a function of Al acceptor concentration.

mechanisms describing the reduction in the ionization energy of impurities have been theoretically considered since the work of Pearson and Bardeen.[21] In a simple model, this reduction is assumed to be caused by the decrease of binding energy which is inversely proportional to the average distance between the impurities. The influence of doping concentration and also compensation on the ionization energy can then be described by the following equation:[21]

$$\Delta E_{\mathrm{i}}(N,K) = \Delta E_{\mathrm{io}} - \alpha(N,K)N^{1/3}, \tag{1}$$

where ΔE_{i} is the ionization energy of the dopant, which depends on the doping concentration (N) and compensation (degree of compensation K), ΔE_{io} corresponds to the ionization energy for very low doping concentration, and α is a factor, which depends on the dielectric constant.[21–23] Scöner *et al.* have experimentally demonstrated that the ionization energy of Al acceptors decreases with increasing the Al acceptor concentration in highly-doped 6H-SiC epitaxial layers and have performed a fit to the experimental data according to Eq. (1) assuming the degree of compensation $K \geqslant 0.3$.[22] Figure 6 shows the calculated ionization energy of Al acceptor in 4H-SiC as a function of the doping concentration, where ΔE_{io} and K are assumed to be 190 meV (Ref. 2) and 0.1, 0.3, and 0.5, respectively. The E_{i} at an Al acceptor concentration of 1×10^{18} cm^{-3} becomes about 180 meV, which agrees well with experimental data reported in the literature.[16] At high concentrations aroung 1×10^{21} cm^{-3}, the E_{i} approaches to zero.

Figure 7(a) shows the acceptor-concentration dependence of the free-hole concentrations at RT. The solid curve depicts the free-hole concentration calculated using the ionization energy of Al acceptor as given in Fig. 6, and the dashed curve is determined by using a constant ionization energy $\Delta E_i = 180$ meV and the degree of compensation $K = 0$. The solid and dashed curves are calculated on the basis of the neutrality equation in Boltzmann approximation. The free-hole concentrations of (0001) samples obtained from Hall-effect measurements are also shown in the figure. For the Al acceptor concentration higher than about 5×10^{20} cm^{-3}, the calculated curves are no longer valid because of invalidity of the Boltzmann approximation ($E_{\mathrm{f}} - E_{\mathrm{v}} < 3kT$, where E_{f}, E_{v}, k, and T are the Fermi enegy, the energy at the top of valence band, the Boltzmann constant,

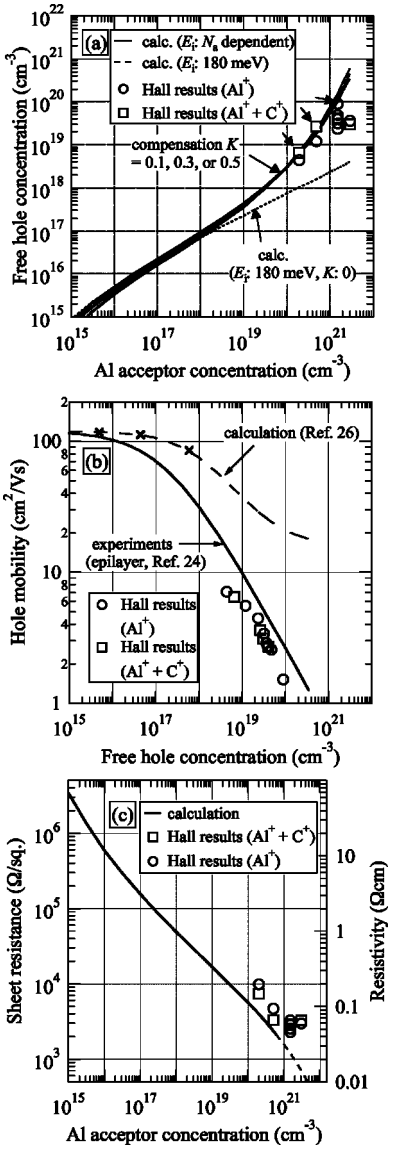

FIG. 7. Al doping-concentration dependence of (a) free-hole concentration, (b) hole mobility, and (c) sheet resistance at RT. Both experimental and calculated properties are shown. The thickness (depth) of implanted layers is assumed to be 0.2 μm.

and temperature, respectively). Therefore, the theoretical expectation is plotted by dotted curves in the region of high-acceptor concentration.

All of the experimental data (see symbols) are located above the dashed curve, indicating that the ionization energy of Al acceptors in those samples is smaller than 180 meV. Two open-square symbols indicated by the arrows for C^+ coimplanted samples (Al concentration of 2×10^{20} cm^{-3} and 5×10^{20} cm^{-3}) take almost the same values as the solid curves. The open-circle symbol (indicated by the arrow) for simple Al^+ implanted and 1 min annealed (Al concentration of 1.5×10^{21} cm^{-3}) also shows a high free-hole concentration. These results demonstrate that optimized implantation and annealing techniques (e.g., C^+ coimplantation or short-time annealing at high temperatures) enhances the probability of Al atoms to occupy Si sublattice sites and reduces implantation-induced defects which may compensate Al acceptors. The other samples shown in Fig. 7(a) show a smaller

free-hole concentration than those three samples mentioned above. In these samples, more implantation-induced defects still remain after annealing process, which compensate Al acceptors.

The dependence of the hole mobility μ on the free hole concentration at RT is shown in Fig. 7(b). The solid line depicts the empirical mobility obtained in Al-doped epitaxial 4H-SiC (0001) in the authors' group.[24] The hole mobility in Al^+-implanted 4H-SiC (0001) samples shows a similar decrease with increasing the free-hole concentration to that in the Al-doped epitaxial samples, although the absolute values of implanted samples are about half as small as the epitaxial samples. The reduced mobility in implanted samples is probably caused by a higher concentration of compensating defects, which behave as scattering centers for free carriers. Stacking faults shown in Fig. 4 may also increase the scattering probability of holes.

Recently the dependence of hole mobility on the free-hole concentration in *p*-type 4H-SiC has been estimated using the following semi-empirical equation[25] by Hatakeyama *et al.*[26] The estimated curve is shown by the dashed curve in Fig. 7(b).

$$\mu = \mu_{\min} + \frac{\mu_{\max} - \mu_{\min}}{1 + \left(\frac{N_d^+ + N_a^-}{N_{\mathrm{ref}}} \right)^{\gamma}}, \tag{2}$$

where $\mu_{\min}$ is the minimum mobility, $\mu_{\max}$ the maximum mobility, N_d^+ the ionized donor concentration, N_a^- the ionized acceptor concentration, N_{ref} the reference concentration, and γ the fitting parameter. Using the parameters as given in Ref. 26, the dashed curve in Fig. 7(b) is obtained. In their report,[26] the parameters in the Eq. (2) have been calibrated by using the three experimental data obtained for epitaxial samples [indicated by crosses in Fig. 7(b)] to apply in the wide range of ionized acceptor concentration. The parameters are the following: $\mu_{\min}$ of 16 cm^2/Vs, $\mu_{\max}$ of 120 cm^2/Vs, N_d^+ of 10^{14} cm^{-3}, N_{ref} of 1.8×10^{18} cm^{-3}, and γ of 0.65.

The dashed curve, however, still takes much higher values than those of both implanted and epitaxial samples, especially in the high free-hole concentration range of $\geqslant 10^{19}$ cm^{-3}. It seems that the estimated values of $\mu_{\min}$ (16 cm^2/Vs) is too high. To obtain a more reasonable analytical expression for the hole mobility, which is applicable for SiC device simulation, more experimental data, especially for high free-hole concentration in the range of 10^{19}–10^{20} cm^{-3} has to be used to adjust the parameters in the semi-empirical equation.

The dependence of the theoretical (solid curve) and experimental (symbols) sheet resistance on acceptor-concentration is shown in Fig. 7(c). The theoretically predicted sheet resistance of 0.2 μm thick *p*-type layers (see solid curve) is obtained with the following assumptions: the concentration of electrically active acceptors corresponds to the concentration of implanted Al atoms, the Al ionization energy depends on acceptor concentration (solid curve in Fig. 7(a) with K of 0.1), and the hole mobility is approximated by the experimental hole mobilities measured in the epitaxial layers.[24]

The experimentally determined sheet resistances are higher than the theoretical curve, which is mainly due to the relatively low mobility in the investigated samples. An improvement of the hole mobility for high-dose Al^+-implanted samples is, therefore, the most important task in order to reduce a sheet resistance. Besides the further increase of mobility, the use of higher implantation energies, which generates deeper *p*-type layers, will help to reduce a sheet resistance.

IV. CONCLUSION

High-dose Al^+ implantation into 4H-SiC (0001) and $(11\bar{2}0)$ has been investigated. The dependence of electrical properties on the implant dose and annealing time were examined by Hall-effect measurements. The Hall data were compared with values calculated using the Al ionization energy which depends on the doping concentration. A low sheet resistance of 2.3 $k\Omega/\square$ (0.2 μm deep) was obtained in (0001) by high-dose Al^+ implantation at 500 °C with a dose of 3.0×10^{16} cm^{-3} and a high-temperature annealing at 1800 °C for a short time of 1 min. In the case of $(11\bar{2}0)$, even room-temperature implantation resulted in a low sheet resistance below 2 $k\Omega/\square$. Free-hole concentrations experimentally obtained were in agreement with the values theoretically expected. On the other hand, hole mobilities did not meet the theoretical expectations. Our discussion clearly reveals that a further decrease of sheet resistances in *p*-type layers can only be achieved via an increase of hole mobility, which may be reached by an improvement of annealing conditions to reduce implantation-induced defects. The optimization of annealing time may be one of the solutions to improve hole mobility.

ACKNOWLEDGMENTS

This work was supported by Grant-in-Aid for JSPS Fellows (for Y.N.), Grant-in-Aid for the 21st Century COE program 14213201, from the Ministry of Education, Culture, Sports, Science, and Technology of Japan, and also by TEPCO Research Foundation (for Kyoto University group).

[1] Yu. A. Vodakov and E. N. Mokhov, *Silicon Carbide 1973* (University of South Carolina, Columbia, S.C., 1974), p. 508.
[2] M. Ikeda, H. Matsunami, and T. Tanaka, Phys. Rev. B **22**, 2842 (1990).
[3] H. Itoh, T. Troffer, and G. Pensl, Mater. Sci. Eng., A **264–268**, 685 (1998).
[4] M. Laube, F. Schmid, G. Pensl, G. Wagner, M. Linnarsson, and M. Maier, J. Appl. Phys. **92**, 549 (2002).
[5] M. A. Capano, R. Santhakumar, R. Venugopal, M. R. Melloch, and J. A. Cooper, Jr., J. Electron. Mater. **29**, 210 (2000).
[6] Y. Negoro, K. Katsumoto, T. Kimoto, and H. Matsunami, J. Appl. Phys. **96**, 224 (2004).
[7] T. Kimoto, A. Itoh, H. Matsunami, T. Nakata, and M. Watanabe, J. Electron. Mater. **25**, 879 (1996).
[8] J. A. Edmond, S. P. Withrow, W. Wadlin, and R. F. Davis, in Interfaces, Superlattices, and Thin Films, edited by J. D. Dow and I. K. Schuller, Mater. Res. Soc. Symp. Proc. No. 77 (Materials Research Society, Pittsburgh, 1987).
[9] T. Kimoto, A. Itoh, H. Matsunami, T. Nakata, and M. Watanabe, J. Electron. Mater. **24**, 235 (1995).

[10]J. W. Palmour, L. A. Lipkin, R. Singh, D. B. Slatter, A. V. Suvorov, and C. H. Carter, Diamond Relat. Mater. **6**, 1400 (1997).
[11]K. Tone and J. H. Zhao, IEEE Trans. Electron Devices **46**, 612 (1999).
[12]H. Yano, T. Hirao, T. Kimoto, H. Matsunami, K. Asano, and Y. Sugawara, IEEE Electron Device Lett. **20**, 611 (2002).
[13]F. Schmid, M. Laube, G. Pensl, G. Wagner, and M. Maier, J. Appl. Phys. **91**, 9182 (2002).
[14]Y. Negoro, N. Miyamoto, T. Kimoto, and H. Matsunami, Appl. Phys. Lett. **80**, 240 (2002).
[15]M. Satoh, Y. Nakaike, and T. Nakamura, J. Appl. Phys. **89**, 1986 (2001).
[16]T. Troffer, M. Schadt, T. Frank, H. Itho, G. Pensl, J. Heindl, H. P. Strunk, and M. Maier, Phys. Status Solidi A **162**, 277 (1997).
[17]Y. Negoro, K. Katsumoto, T. Kimoto, and H. Matsunami, Mater. Sci. Forum **457–460**, 933 (2004).
[18]R. Kumar, J. Kojima, and T. Yamamoto, Jpn. J. Appl. Phys., Part 1 **39**, 2001 (2000).
[19]H. Tanaka, S. Tanimoto, M. Yamanaka, and M. Hoshi, Mater. Sci. Forum **389–393**, 803 (2002).
[20]N. T. Son, P. N. Hai, W. M. Chen, C. Hallin, B. Monemar, and E. Janzén, Phys. Rev. B **61**, 10544 (2000).
[21]G. L. Pearson and J. Bardeen, Phys. Rev. **75**, 865 (1949).
[22]A. Schöner, N. Nordell, K. Rottner, R. Helbig, and G. Pensl, Inst. Phys. Conf. Ser. **142**, 493 (1996).
[23]B. I. Shklovskii and A. L. Éfros, Sov. Phys. Semicond. **14**, 487 (1980).
[24]H. Matsunami and T. Kimoto, Mater. Sci. Eng., R. **20**, 125 (1997).
[25]D. M. Caughey and R. E. Thomas, Proc. IEEE **55**, 2192 (1967).
[26]T. Hatakeyama *et al.*, Mater. Sci. Forum **433–436**, 443 (2003).